

# Vortices in Superfluid Fermi Gases

Yiruo Lin

December 16, 2008

## Abstract

I briefly reviewed vortex properties and its formation in ultra-cold Fermi gases. For the problem of vortex structure, I focused on mechanisms of density depletion in the vortex core, which is relevant to experiment.

## Introduction

Ultra-cold atomic gases provide us excellent physics systems in which we could study many-body physics in a controllable way, thanks to the extraordinary progress made by atomic physicists. In the case of Fermi gases, by tuning interactions among atoms experimentally, we can get systems from BEC limit all the way to BCS limit continuously. Studying this BEC-BCS crossover can shed light on many areas of interest to us, such as high temperature superconductivity.

Superfluidity is one of the most important properties in the ultra-cold Fermi gases. Presence of vortices is the most unambiguous evidence for superfluidity. However, unlike Bose gases, which show significant density depletion in the vortex core; the Fermi gases are not expected to show such density variations, at least in the BCS limit. This makes it challenging to detect vortices in Fermi gases directly in experiment. There's been theoretical work (for example, [1, 2, 3, 4]) indicating appreciable density depletion in vortex cores in the strong coupling regime which may be experimentally detected. In 2005, an experiment group at MIT, Zwierlein et al. [5] provided direct observation of vortices in a strongly interacting Fermi gas. Following this ground-breaking work, further theoretical work has been done to study vortex structures in more details and in new Fermi systems (for example, [6] [7]).

## Preliminary on ultra-cold Fermi gases

In order to discuss vortices in Fermi gases, it's necessary to have a basic picture of the relevant physics systems in question. I would mainly follow discussions of Leggett [8] and Sa de Melo [9]. The systems we are dealing with here are Fermi alkali gases of  $^{40}K$  and  $^6Li$ . We will consider systems of two hyperfine species, denoted in pseudo spin notation as  $|\uparrow\rangle$  (spin up) and  $|\downarrow\rangle$  (spin down). They can be trapped in a magnetic field due to interaction with magnetic field. Since their energies depend on magnetic field, we could use magnetic field to tune effective interactions between the two hyperfine species. Recently experiments

use laser trapping to trap Fermi atoms, while magnetic field is used to tune the effective interaction strength between two hyperfine species. The raw data in experiments reduces to a measurement of density of the system as a function of space and possibly time.

The interaction between two species is characterized by scattering length. Since we are studying dilute Fermi gas ( $kr_0 \ll 1$ ,  $k$  is wave vector of relative wavefunction of two atoms,  $r_0$  is typical interaction range), we only need to consider s-wave scattering to a good approximation (so that there's only interaction between different spins). In a two-body interaction problem in the single-channel (i.e. the two atoms interact in a fixed interatomic potential), the s-wave scattering length  $a_s$  is negative and proportional to  $\delta^{-1}$  ( $\delta \equiv V - V_c$ ,  $V_c$  is critical depth of potential well) if the interatomic potential is just too weak to tolerate bound state and becomes positive and proportional to  $\delta^{-1}$  if there's just a bound state. In a Feshbach resonance, two channels are coupled and scattering length goes from negative to positive as magnetic field is swept through resonance (see Fig 1). For our purposes, it is sufficient to think the system in a harmonic trap with tunable interaction between different species which is controlled by magnetic field. Crudely speaking, the interaction strength between atoms can be characterized by a dimensionless variable  $1/k_F a_s$  in a many-body Fermi system, where  $k_F$  is Fermi momentum for a noninteracting Fermi system.  $1/k_F a_s < 0$  corresponds to BCS regime and  $1/k_F a_s \rightarrow -\infty$  as attractive interaction becomes weak and approaches weak-coupling BCS limit.  $1/k_F a_s > 0$  corresponds to BEC regime and  $1/k_F a_s \rightarrow +\infty$  as attraction becomes strong and approaches tight binding BEC molecule limit. At  $1/k_F a_s = 0$ , the scattering length diverges (but no physical singularity) and we are in unitary limit where real bound state in free space is about to exist. Figure 2 shows a cartoon picture of phase diagram of the Fermi system.

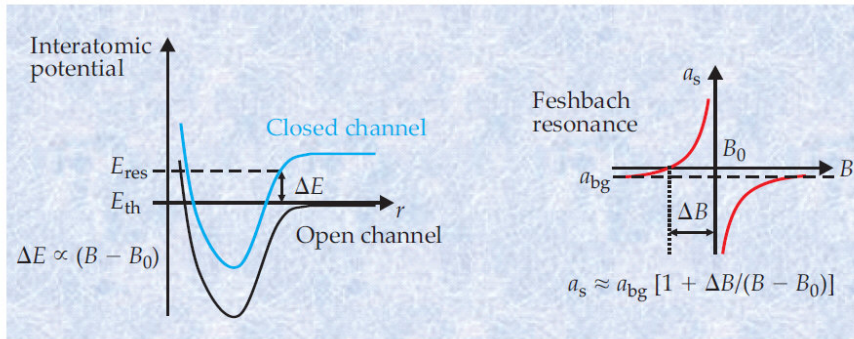


Figure 1: Feshbach resonances,  $B_0$  is resonance magnetic field,  $\Delta B$  is resonance width,  $a_{bg}$  is background scattering length (the scattering length in the open channel without coupling to the closed channel). Fig. from [9]

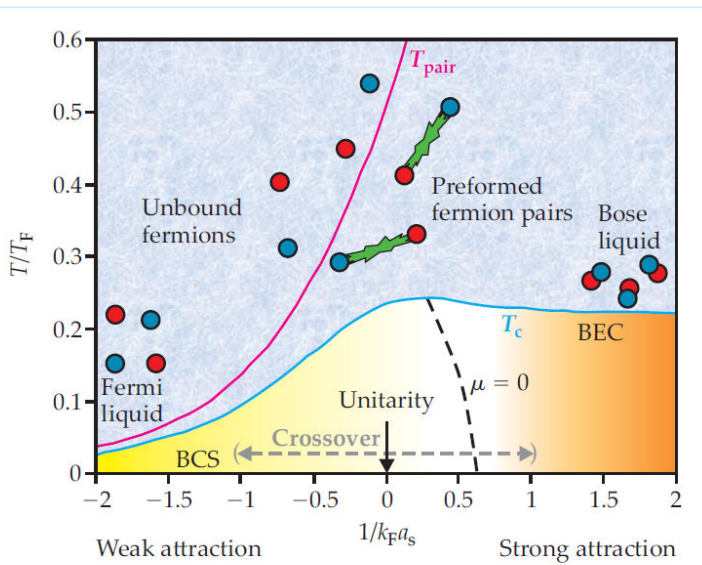


Figure 2: Phase diagram of Fermi superfluid cross Feshbach resonance,  $T_F$  is Fermi temperature,  $T_c$  is transition temperature at which the system becomes superfluid. Fig. from [9]

## Vortex structure through Feshbach resonance

As is noted in the introduction, we expect to observe vortices in strongly interacting Fermi gases due to density depletion in vortex cores. Indeed, vortices were observed by Zwierlein et al.[5] in a strongly interacting Fermi gas near a Feshbach resonance. Fig 3 shows vortex lattices in the BEC-BCS crossover, where little black solid circles are vortex cores where particle density is lower than the bulk density.

Now Let's turn to quantitative description of vortices, in particular cross a Feshbach resonance. We will focus on a single vortex in the  $T = 0$  limit, which is relatively well studied. First question concerns with the energy of a vortex and the corresponding critical velocity for its formation. In the weak-coupling BCS limit, a general analysis [10] from kinetic energy associated with a vortex of circulation quanta  $\kappa$  and loss in condensation energy in the vortex core of range  $\xi_{BCS}$  shows that the energy is similar to that of a Bose system with a BCS coherence length.

$$E \simeq \frac{\pi \kappa^2 \hbar^2 n_\sigma}{2m_a} \ln\left(D \frac{R_c}{\kappa \xi_{BCS}}\right) \quad (1)$$

where  $D$  is a constant of order one,  $R_c$  is radius of the trapped gas in a cylinder,  $n_\sigma$  is number density of each spin.

It's clear from this equation that a vortex with  $\kappa > 1$  would break into several vortices with unit circulation to lower the total energy. The point here is that the condensation energy is negligible and the result is similar to that of a Bose system, for example,  $^4He$ . The corresponding critical velocity for a vortex formation is rather small since it is given by the

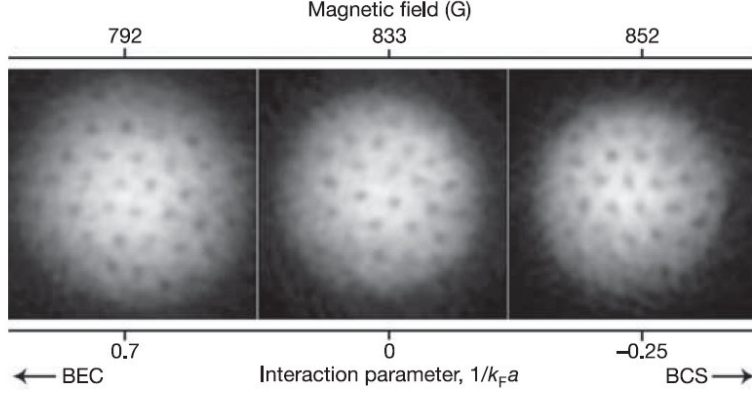


Figure 3: Vortex lattices in the BEC-BCS crossover. Fig. from [5]

ratio of energy to angular momentum, the former scales as  $N_\sigma^{2/3}$  while the latter scales as  $N_\sigma$ . The form of energy of a vortex in equation 1, in particular its dependence on length scale  $\xi_{BCS}$  was confirmed by Nygaard et al.[11] by solving BdG equations numerically. It was also mentioned that there's different length scales in gap function around the vortex core. Since the work was in the weak-coupling limit, density near a vortex core shows no significant difference from bulk value as expected.

Bulgac and Yu [1] showed a large density depletion at vortex core in unitary limit by solving BdG equations numerically, assuming gap function and quasiparticle wavefunctions according to a single vortex with unit circulation. Machida and Koyama [2], Kawaguchi and Ohmi [3] explained density depletion due to coupling of fermionic atoms and BEC molecules using fermion-boson coupling model. The Hamiltonian used in [2] is given by

$$H_{BF} = \int dr [\Phi_\sigma^\dagger(r) (-\frac{1}{2m} \nabla^2 - \mu) \Phi_\sigma(r) - U \Phi_\uparrow^\dagger(r) \Phi_\downarrow^\dagger(r) \Phi_\downarrow(r) \Phi_\uparrow(r)] \quad (2)$$

$$+ \phi_B^\dagger(r) (-\frac{1}{4m} \nabla^2 + 2\nu - 2\mu) \phi_B(r) + g(\phi_B^\dagger(r) \Phi_\downarrow(r) \Phi_\uparrow(r) + h.c.) \quad (3)$$

where  $\Phi_\sigma$  and  $\phi_B$  are the field operators for atoms and molecules, respectively.  $2\nu$  is the energy of a molecule relative to that of two atoms,  $\mu$  is the chemical potential.  $U$  is coupling constant between atoms and  $g$  is coupling strength between atoms and molecules, which is significant near Feshbach resonance. In the mean field approximation, the gap functions are defined as

$$\phi^B(r) = g \langle \phi_B(r) \rangle \quad (4)$$

$$\Delta^F(r) = U \langle \Phi_\downarrow(r) \Phi_\uparrow(r) \rangle \quad (5)$$

In the generalized BdG equations, the effective off-diagonal potential becomes  $\Delta^F(r) + \phi^B(r)$ . Similarly, an equation for  $\phi^B(r)$  is obtained by the equilibrium condition  $i\hbar < \partial\phi_B(r)/\partial t > = < [\phi_B(r), H] > = 0$ ,

$$\left[-\frac{1}{4m} \nabla^2 + 2\nu - 2\mu\right]\phi_B(r) = \frac{g^2}{U}\Delta^F(r) \quad (6)$$

In [2], BdG equation was solved numerically in a self-consistent way with BCS gap equation and number conservation constraint (total number of particles is the sum of the number of the atoms and twice the number of the molecules) on chemical potential. No trapping potential was included since the vortex core is much smaller than condense size and is not qualitatively affected by a trapping potential. The density distribution for different  $\nu$  are shown in figure 4. For smaller  $\nu$ , which corresponds to region closer to Feshbach, we see clear density depletion and a much larger ratio of molecules. We also note that not only for molecule, the atomic density distribution also shows BEC-like behavior near resonance. This result is consistent with that of [3], in which similar equations were used with some minor variations. In that letter, the total number of atoms and molecules were found to cross in the resonance region (see figure 5), consistent with our expectation. From the number density distributions (see figure 6), we see that as the system goes from BCS to BEC, both atom and molecule density distribution around the vortex core become BEC like. Hence the strong density depletion at BEC-BCS crossover is from both atom and molecule density depletion.

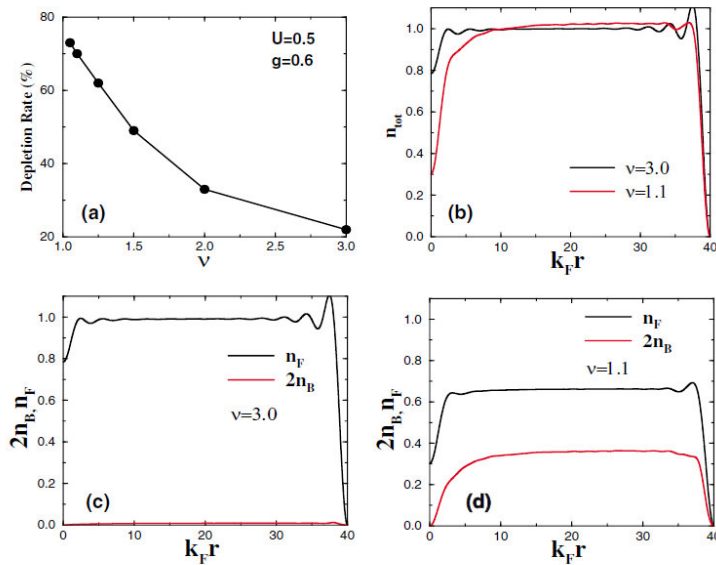


Figure 4: Density distribution for different  $\nu$ .  $n_B$ ,  $n_F$  are number density for boson (fermion molecule) and fermion respectively. Fig. from [2]

Chien et al. [4] solved BdG equations numerically and examined local fermionic density of states  $N(E, r) = \sum_n [u_n^2 \delta(E - E_n) + v_n^2 \delta(E + E_n)]$ , where  $E_n$  are eigenvalues of BdG equations and  $u_n$ ,  $v_n$  eigenfunctions. They ascribed density depletion at crossover to change

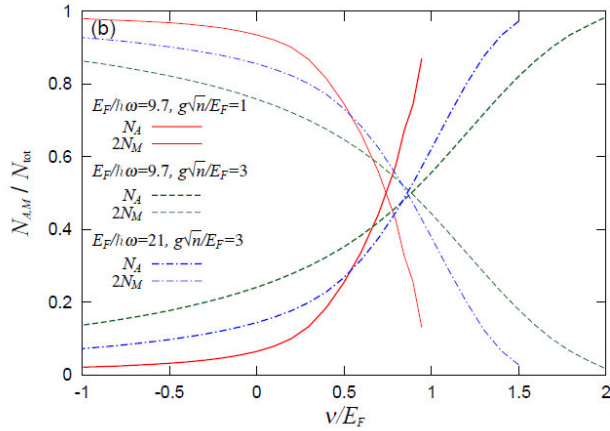


Figure 5: Total number of atoms and molecules as function of  $\nu/E_F$  and for particle number and coupling strength. Fig. from [3]

of core excitation spectra (integral of  $N(E, r)$  over negative  $E$  reflects density distribution inside the core), as shown in figure 7.

Sensarama et al. [6] studied vortex structure through the BEC to BCS crossover in details. They found two length scales for gap function on the BCS side, while only one length scale outside the BCS region (see figure 8). They also discussed other interesting properties about circulating current (which maximizes at unitarity) and fermionic bound states in the vortex core, which exist even in the bosonic regime, unique to bosonic BEC.

So far, most work has focused on single vortex properties at zero temperature. More work for generalized situations is needed to gain more complete knowledge of vortex structure. On the other hand, very recently, there's a lot of interest in new systems such as spin polarized and mass-imbalanced Fermi systems. Understanding vortex behaviors and superfluidity in them is called for. For example, Iskin [7] studied numerically vortex core states of mixture of  ${}^6\text{Li}$  and  ${}^{40}\text{K}$  at  $T = 0$  and he found that vortex core is mostly occupied by light atoms  ${}^6\text{Li}$ , while  ${}^{40}\text{Li}$  is highly depleted at the vortex core.

## Vortex formation in a rotating Fermi gas

Now let's turn to the question of vortex formation. I'll follow the work by Tonini et al. [12]. They considered 2D two-spin Fermi gases in a rotating harmonic trap and also 3D unitary Fermi gases. They showed that vortex free gases in both cases are subject to a dynamic instability for fast enough rotation. They then verified 2D case by numerical simulation of BdG equations.

The stability analysis is based on hydrodynamic theory of superfluid. Introduce the phase of order parameter  $S(r, t)$  so that the velocity field is  $v = \nabla S/m$ . In the rotating frame, the

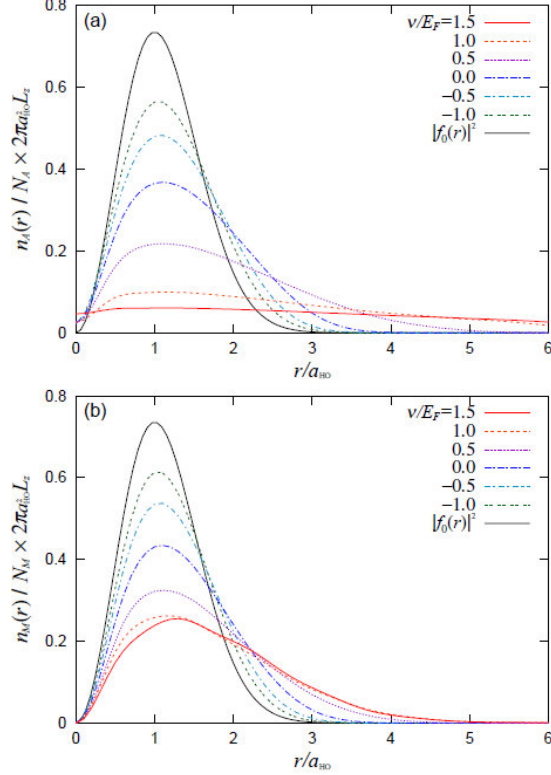


Figure 6: Density distribution for different  $\nu/E_F$ .  $|f_0(r)|^2$  is the density distribution of a noninteracting BEC. Fig. from [3]

hydrodynamic equations read

$$\partial_t \rho = -\nabla \cdot [\rho(v - \Omega(t) \times r)] \quad (7)$$

$$-\partial_t S = \frac{1}{2} m v^2 + U(r) + \mu_0[\rho(r, t)] - \mu - m(\Omega(t) \times r) \cdot v \quad (8)$$

where  $\Omega(r, t)$  is angular velocity along the rotation axis  $z$ ,  $U = \frac{1}{2} m \omega^2 [(1-\epsilon)x^2 + (1+\epsilon)y^2]$  is the 2D harmonic trap potential,  $\epsilon > 0$  measures its anisotropy. The first equation is just the continuity equation in the rotating frame, the second equation is basically Euler's equation. These equations are valid for slowly varying density and phase in space (compared to the size of a Cooper pair) and time (compared to  $\hbar/\Delta$ ). Assuming the rotation frequency is increased slowly enough so that the density and the phase follow vortex free stationary states adiabatically. Now first solve stationary state solution (rotation free) of equation 7 and 8, and then perform a linear stability analysis of the stationary solution. In the 2D case, take the ansatz for the phase:  $S(r) = m\omega\beta xy$ , which is consistent with the harmonic trap. The stationary solution obeys

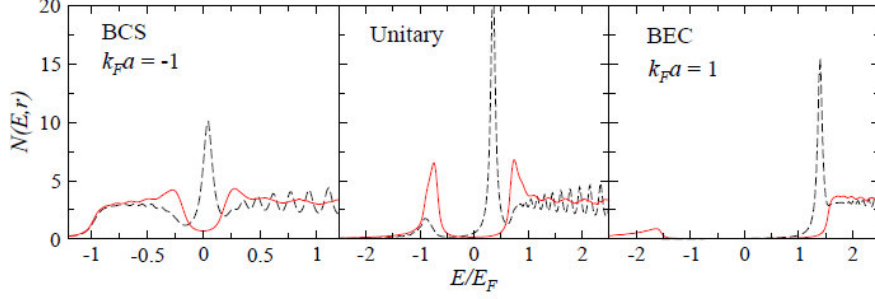


Figure 2: Local fermionic density of states  $N(E, r)$  as function of  $E$  for BCS ( $k_F a \approx -1$ ), unitary and BEC ( $k_F a \approx 1$ ) cases, at the center  $r = 0$  (black dashed curves) and radius  $r = 25/k_F$  (red solid curves) of the vortex core. The bulk value of the gap  $\Delta_\infty$  is  $0.21, 0.68, 1.3E_F$ , respectively. In the BEC case,  $\mu \approx -0.8E_F$ . Here  $E_F$  is the noninteracting Fermi energy at the trap center.

Figure 7: Fig. from [4]

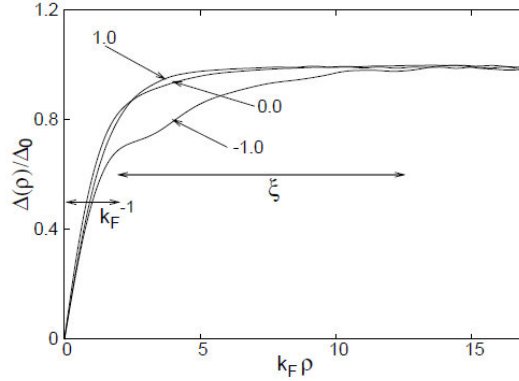


FIG. 1: The order parameter normalized by its value far from the vortex for three different couplings  $1/k_F a_s = -1, 0, 1$ . Note the clear emergence of two length scales in the BCS limit  $1/k_F a_s = -1$ .

Figure 8: Fig. from [6]

$$\beta^3 + \left(1 - 2\frac{\Omega^2}{\omega^2}\right)\beta - \epsilon\frac{\Omega}{\omega} = 0 \quad (9)$$

The stationary solution follows the upper branch of solution, corresponding to the stirring procedure considered here (slowly increasing rotation velocity from zero). Then one performs a linear stability analysis around this stationary solution and finds the region of dynamic instability corresponding to positive imaginary Lyapunov exponents. Figure 9 shows instability domain in the  $\Omega - \epsilon$  plane for different degrees of polynomials (the form of  $\delta\rho(r)$  and  $\delta S(r)$ ). The critical frequency of the first significant instability is around  $0.8\omega$  for  $\epsilon = 0$ . In the 3D unitary limit, the exact equation of state is known so that a similar analysis can be



done and the resulting instability domain is more complicated than in 2D.

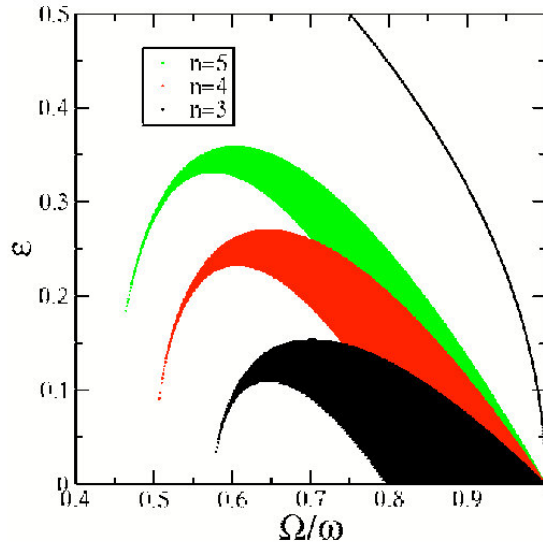


FIG. 2: For the upper branch of solution for the phase parameter, in 2D: Dark areas: instability domain in the  $\Omega - \epsilon$  plane for degrees  $n$  equal to 3, 4 and 5 (crescents from bottom to top). There is no dynamical instability for  $n \leq 2$ . Solid line: border  $\Omega^2 = (1 - \epsilon)\omega$  of the branch existence domain.

Figure 9: Fig. from [12]

To check whether a dynamic instability results in formation of vortices, numerical solutions of 2D Fermi gas were found by solving time-dependent "BdG" equations. It was found that abrupt and disordered entrance of vortices occurs (for  $\epsilon = 0.1$ ) when  $\Omega \geq 0.7$ , consistent with  $n = 3$  instability mode where a significant Lyapunov exponent is obtained for  $\Omega > 0.68\omega$  (refer to figure 9). After the turbulence is settled, a stable vortex lattice forms (see figure 10).

## Summary

I have discussed vortex structure and vortex formation in a ultra-cold Fermi gas at zero temperature. Properties of a single vortex in a Fermi gas at zero temperature are quite well understood. In particular, density depletion mechanisms in the crossover regime have been confirmed and extensively studied. From above discussions, we can conclude that a significant density depletion in the crossover regime is due to interplay of fermionic atoms and BEC molecules and the density distribution assembles that of a true Bose system. Vortex formation in a rotating trap is due to a dynamic instability of hydrodynamic nature triggered by the rotating trap, which is confirmed numerically in 2D. Obviously, further studies are needed to extend to more general situations. Also, exciting physics in newly studied systems, such as spin polarized and mass-imbalanced Fermi gases awaits us (see [9]).

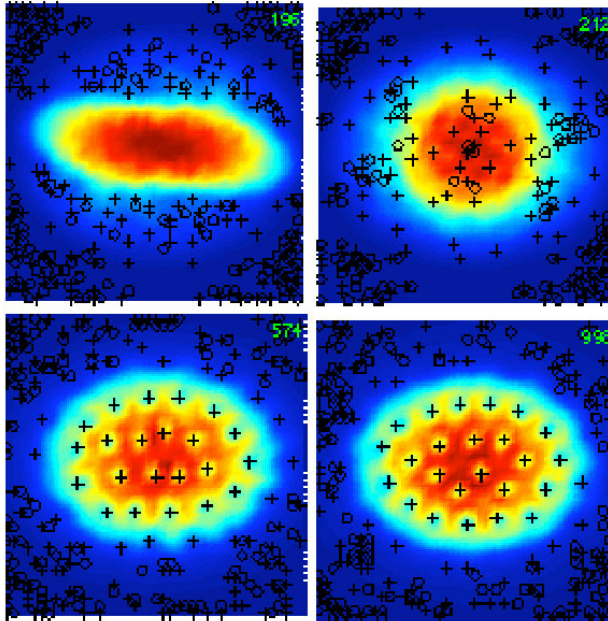


Figure 10: Trap anisotropy  $\epsilon = 0.1$ . Crosses: positive charge vortices. Circles: negative charge vortices. Time is in unit of  $\omega^{-1}$ , final rotation velocity  $\Omega = 0.8\omega$ . Fig. from [12]

## References

- [1] A.Bulgac and Y. Yu, Phys. Rev. Lett. 91, 190404 (2003)
- [2] M. Machida and T. Koyama, Phys. Rev. Lett. 94, 140401 (2005)
- [3] Y. Kawaguchi and T. Ohmi, arXiv:cond-mat/0411018v2 [cond-mat.soft] 5 Apr 2005
- [4] C Chien et al. arXiv:con-mat/0510647v2 [cond-mat.supr-con] 26 Oct 2005
- [5] M.W. Zwierlein et al. Nature 435, 1047 (2005)
- [6] R. Sensarma, M. Randeria and TL. Ho arXiv:con-mat/0510761v1 [cond-mat.supr-con] 27 Oct 2005
- [7] M. Iskin, Phys. Rev. A 78, 021604 (2008)
- [8] A.J. Leggett, Quantum Liquids (Oxford, 2006)
- [9] CAR. Sa de Melo Physics Today 45, Oct. 2008
- [10] G.M. Bruun and L. Viverit, arxiV:cond-mat/0106011v1 1 Jun 2001
- [11] N. Nygaard et al. arXiv:cond-mat/0210526v2 [cond-mat.soft] 16 Apr 2003
- [12] G. Tonini, F. Werner and Y. Castin, arXiv:cond-mat/0504612v2 [cond-mat.other] 21 Feb 2006